

Comparative study on internal friction in an Al-Pd-Mn icosahedral quasicrystal and its crystal approximants

Yeong-Gi So,^{1,*} Shun Sato,¹ Keiichi Edagawa,¹ Takahiro Mori,² and Ryuji Tamura²

¹*Institute of Industrial Science, The University of Tokyo, Komaba, Meguro-ku, Tokyo 153-8505, Japan*

²*Department of Materials Science and Technology, Tokyo University of Science, Yamazaki, Noda-shi, Chiba 278-8510, Japan*

(Received 11 November 2009; revised manuscript received 21 November 2009; published 31 December 2009)

The internal friction was measured for an Al-Pd-Mn icosahedral phase (i-phase) and its 1/1 and 2/1 approximant phases in an Al-Pd-Mn-Si system in a forced flexural-oscillation mode in a frequency range of 0.05–20 Hz and a temperature range of 300–873 K. For the i-phase, large and small absorption peaks were observed with $Q^{-1} \approx 1.3 \times 10^{-2}$ and 8×10^{-4} , respectively. These two peaks were absent for the 1/1-phase, which showed two other peaks instead. The 2/1-phase exhibited the features of both the i and 1/1-phases; it showed two peaks of the i-phase and one of the two peaks of the 1/1-phase. All the observed peaks were of the thermally activated relaxation type, and their activation enthalpies and frequency factors were evaluated. The larger peak of the i-phase, which was absent for the 1/1-phase and present with a much reduced intensity for the 2/1-phase, was shown to result from a relaxation process involving collective atomic motion. Collective and correlated phason jumps were discussed as a possible mechanism for it. It was speculated that the other peaks observed only for the approximant phases are due to Zener relaxations by the reorientation of atom pairs involving Si.

DOI: [10.1103/PhysRevB.80.224204](https://doi.org/10.1103/PhysRevB.80.224204)

PACS number(s): 61.44.Br, 62.40.+i

I. INTRODUCTION

Quasicrystals have a peculiar type of ordered structure characterized by crystallographically disallowed point-group symmetry and by quasiperiodic translational order.^{1–3} Since the discovery of a quasicrystal in a rapidly quenched Al-Mn alloy,⁴ such quasicrystalline phases have been found in various metallic alloy systems.⁵ Their atomic structure, stability, and physical properties including elastic properties have attracted much attention, and many studies have so far been carried out to clarify them.

Originating in the quasiperiodic translational order, quasicrystals have a special type of elastic degrees of freedom termed as phason degrees of freedom.^{3,6} Quasicrystals are accompanied by the phason elastic field in addition to the phonon (conventional) elastic field. The generalized elasticity of quasicrystals is described in terms of these two types of elastic fields.^{7–9} Within linear elasticity, the elastic energy of quasicrystals consists of the following three types of quadratic terms: phonon-phonon, phason-phason, and phonon-phason terms. Correspondingly, the elasticity of quasicrystals comprises the following three components: pure phonon elasticity, pure phason elasticity, and phonon-phason coupling.

The hydrodynamic theory of quasicrystals predicts diffusive phason modes,^{9,10} where phason waves decay exponentially in time with a characteristic time proportional to λ^2 (λ : the phason wavelength). In fact, phason waves or phason fluctuations in quasicrystals are accompanied by collective atomic jumps and their relaxation proceeds with a slow diffusive process involving thermally activated atomic jumps. Francoual and her co-workers¹¹ have investigated the dynamics of phason modes in i Al-Pd-Mn by coherent x-ray scattering and time-correlation spectroscopy. They observed the expected λ -dependent decay of phason waves with decay times ranging from 20 to 70 s at 923 K and estimated the activation enthalpy to be 3 ± 1 eV. In general, when a dis-

location moves in quasicrystals, a highly localized phason strain termed phason wall is left behind. Feuerbacher and his co-workers¹² have observed by *in situ* transmission electron microscopy (TEM) the relaxation process of the phason wall in i Al-Pd-Mn. They reported the relaxation times ranging from 0.3 to 2×10^4 s, obeying an Arrhenius temperature dependence with an activation enthalpy of 4 eV and a frequency factor of 4×10^{21} s⁻¹. Phason fluctuations or phason-strain relaxations in Al-Cu-Co decagonal quasicrystals have been observed by Edagawa *et al.*^{13–15} by *in situ* high-resolution TEM, and characteristic times ranging from 10 to 700 s have been reported at high temperatures of around 1123 K.

In the presence of phonon-phason coupling, propagating phonon waves should couple with damping phason waves, resulting in the generation of the internal friction. Rochal and Lorman have theoretically discussed the internal friction induced by phonon-phason coupling.¹⁶ Experimentally, the internal friction of icosahedral quasicrystals was first measured in i-Al-Pd-Mn single-crystal samples by Feuerbacher *et al.*¹⁷ They observed two major peaks, which were attributed to two different phason relaxation mechanisms, i.e., those involving local individual phason jumps and collective correlated phason jumps, respectively.^{12,17} It has been shown that the activation parameters in the latter agree well with those evaluated for the relaxation processes of the phason wall in i Al-Pd-Mn by Feuerbacher *et al.*¹² and of the phason waves in i Al-Pd-Mn by Francoual *et al.*¹¹

Crystal approximants^{18–20} to a quasicrystal are the crystalline phases whose local structure is similar to that of the quasicrystal. These crystal approximants have played important roles in the investigations of the physical properties of quasicrystals. For example, de Boissieu and his co-workers²¹ have conducted a comparative study on the diffuse scattering in the Zn-Mg-Sc i-phase and its 1/1 crystal approximant in the Zn-Sc system. It was shown that the diffuse scattering attributed to long-wavelength phason modes was observed

only for the *i*-phase, which indicates that the phason modes are characteristic of the quasiperiodic long-range order. In this paper, we report on a comparative study on the internal friction of an Al-Pd-Mn *i*-phase and its 1/1 and 2/1 approximant phases in the Al-Pd-Mn-Si system, mainly focusing on the relaxations related to the phason modes.

II. EXPERIMENTAL PROCEDURES

Mother alloy ingots with nominal compositions of Al₇₃Pd₁₉Mn₈ for the *i*-phase, Al_{67.5}Pd_{11.5}Mn_{14.5}Si_{6.5} for the 1/1-phase, and Al_{69.5}Pd_{23.0}Mn_{6.2}Si_{1.3} for the 2/1-phase were synthesized from pure Al (99.999 wt %), Pd (99.95 wt %), Mn (99.99 wt %), and Si (99.999 wt %) by arc melting under an argon atmosphere.

For the *i*-phase, the mother alloy ingots were packed into an alumina crucible with a diameter of 16 mm and subsequently sealed in an evacuated silica tube. A large single crystal of the *i*-phase was grown by a Bridgman technique with a growth speed of 2 mm/h. Single-crystal samples with a length of approximately 40 mm were reproducibly obtained. The crystallographic orientations of the ingots were characterized by backscattering x-ray Laue diffraction measurements. The absence of precipitates of the contaminant phases and the homogeneity of the sample were confirmed by powder x-ray diffraction measurements and scanning electron microscopy with energy dispersion spectroscopy (EDS). The typical composition shown by EDS was Al_{69.5}Pd_{21.0}Mn_{9.5}. The single-crystal sample was cut and shaped into a rectangular parallelepiped with the three edges of $|\mathbf{a}|=35$ mm, $|\mathbf{b}|=4$ mm, and $|\mathbf{c}|=1$ mm for the internal friction measurements. Here, we prepared three types of samples with different crystallographic orientations: one was a sample with the longitudinal direction \mathbf{a} parallel to a two-fold axis, another with \mathbf{a} parallel to a fivefold axis, and the other with \mathbf{a} parallel to a threefold axis. In all three samples, the normal direction \mathbf{c} to the largest face was parallel to a twofold axis. We hereafter call the three samples the twofold, fivefold, and threefold samples, respectively. Some pieces of the single crystal of the *i*-phase were crushed and powdered, and this powder was used to produce sintered alloys of the *i*-phase were produced by plasma-activated sintering (PAS).

For the 1/1 and the 2/1 approximant phases, the mother alloy ingots were sealed in an evacuated silica tube and annealed at 1073 K for 25 h, followed by water quenching. Annealed alloys were subsequently crushed and powdered, and sintered polygrained samples of the 1/1-phase and 2/1-phase were produced by PAS. The x-ray diffraction spectra were measured for all the three sintered polygrained samples. They were cut and shaped into rectangular parallelepipeds with the same size as that of the single-crystal *i*-phase sample for the internal friction measurements.

Internal friction measurements were carried out in a forced flexural-oscillation mode using a dynamical mechanical analyzer. Here, one end of the sample is clamped and an oscillating force is applied in the \mathbf{c} direction at the other end to provide oscillating flexural stress to the sample. In this configuration, an oscillating tension-compression stress is applied along the \mathbf{a} direction, i.e., along the n -fold directions

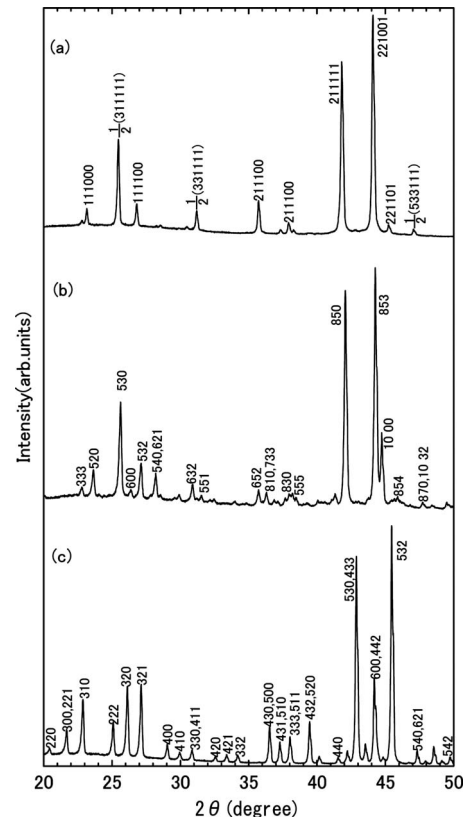


FIG. 1. X-ray diffraction spectra for the polygrained samples of (a) *i*-Al-Pd-Mn, (b) the 2/1, and (c) 1/1 approximant phases in the Al-Pd-Mn-Si system.

for the n -fold samples ($n=2, 5$, or 3). The induced flexural displacement was monitored to evaluate the internal friction Q^{-1} . The displacement showed an oscillation with the same frequency as that of the applied stress but exhibited a phase shift δ due to anelasticity. The internal friction is given by $Q^{-1}=\tan \delta$. The measurements were performed in a temperature range of 300–873 K in air at a heating rate of 2 K/min and a frequency range 0.05–20 Hz. The strain amplitudes used in the measurements were 10^{-5} for the single-crystal samples and 10^{-4} for the polygrained samples.

III. RESULTS

Figures 1(a)–1(c) show the x-ray diffraction spectra for the polygrained samples of the *i*, 2/1, and 1/1-phases, respectively. Here, the indexing scheme of Elser²² is used for the *i*-phase. The indices for the 1/1-phase are from the paper by So *et al.*,²³ and those for the 2/1-phase are calculated from the indices of the *i*-phase, according to the paper by Koshikawa *et al.*²⁴ We find no appreciable amount of contaminant phases in any of the three samples. The six-dimensional lattice constant a_0 of the *i*-phase was evaluated to be 0.647 nm. The lattice constants $a_{1/1}$ and $a_{2/1}$ for the 1/1 and 2/1-phases were evaluated to be 1.229 and 2.024 nm, respectively. These values are slightly lower than those calculated from a_0 : $a_{1/1}=a_0 2^{1/2}(\tau+2)^{-1/2}$, $\tau^2=1.259$ nm and $a_{2/1}=a_0 2^{1/2}(\tau+2)^{-1/2}$, $\tau^3=2.038$ nm [$\tau=(1+\sqrt{5})/2$]. This is

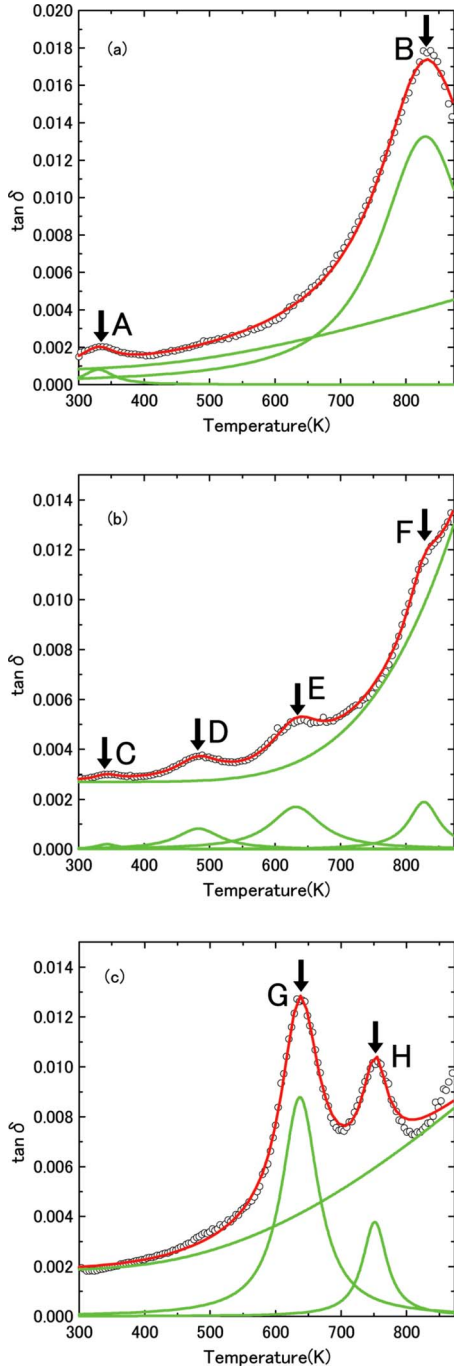


FIG. 2. (Color online) Temperature dependences of the internal friction for the polygrained samples of (a) i Al-Pd-Mn, (b) the 2/1, and (c) 1/1 approximant phases in the Al-Pd-Mn-Si system at a frequency of 0.1 Hz. Open circles represent the experimental data. Solid lines represent the results of the fitting: the sum of the HTDB component and Lorentz functions representing the peaks. The individual components of the HTDB and Lorentz functions are also shown in the figures.

because the approximant phases contain Si, which has a relatively small atomic size.

Figures 2(a)–2(c) show the temperature dependences of the internal friction for the polygrained i, 2/1, and 1/1-phases, respectively, at a frequency of 0.1 Hz. For the i-phase

in (a), two peaks, one small and one large, are observed at around 330 and 830 K, respectively, which are designated as A and B, respectively. For the 2/1-phase in (b), four small peaks, designated as C, D, E, and F, can be identified; they appear to be added to the component that increases significantly with increasing temperature in a high-temperature region. This type of background component of internal friction is often observed in various metallic alloys, and it is sometimes called the “high-temperature damping background (HTDB) (Ref. 25).” Although the origin of the HTDB has not been fully clarified, its temperature dependence $Q_{\text{HTDB}}^{-1}(T)$ is often expressed as²⁶

$$Q_{\text{HTDB}}^{-1}(T) = A + B \exp\left(\frac{-C}{k_{\text{B}}T}\right), \quad (1)$$

where A , B , and C are arbitrary constants, and k_{B} is the Boltzmann constant. The 2/1-phase data shown in Fig. 2(b) are fitted to the sum of $Q_{\text{HTDB}}^{-1}(T)$ in Eq. (1) and four Lorentz curves for the four peaks to determine the net Q^{-1} values for the four peaks. The results of this fitting (the total Q^{-1} , Q_{HTDB}^{-1} , and four Lorentzians) are shown in the figure. The i-phase data shown in Fig. 2(a) are also fitted to the sum of the HTDB component and the Lorentz curves. Here, we had quite a large ambiguity in determining the HTDB component because the high-temperature side of peak B was not fully observed. The temperature dependence of Q^{-1} for i Al-Pd-Mn was measured previously by Feuerbacher *et al.*¹⁷ up to 1100 K, in which peaks A and B were observed. In their data, the high-temperature side of peak B was fully observed, with the Q^{-1} value going down to approximately 20% of the peak height at around 1000 K. We took this fact into consideration to determine the HTDB component, as shown in Fig. 2(a). In the 1/1-phase data shown in Fig. 2(c), two large peaks are observed at around 630 and 750 K, which we designated as G and H, respectively. Here, the above-described data fitting was again conducted. In Figs. 2(a)–2(c), the following pairs of peaks are at approximately the same temperature: (A and C), (B and F), and (E and G).

For the i-phase, the positions of peaks A and B shift with changes in the frequency f , as shown in Figs. 3(a) and 4(a). Here, they shift toward a high temperature with increasing frequency, suggesting that the two peaks originate in thermally activated relaxation processes. In general, the relaxation time τ of a thermally activated relaxation process can be given by

$$\tau^{-1} = \tau_0^{-1} \exp\left(\frac{-H}{k_{\text{B}}T}\right), \quad (2)$$

where τ_0^{-1} is the frequency factor and H is the activation enthalpy. The peak temperature T_{P} is given by the condition $2\pi f\tau = 1$, leading to the relation

$$f = \frac{1}{2\pi} \tau_0^{-1} \exp\left(\frac{-H}{k_{\text{B}}T_{\text{P}}}\right). \quad (3)$$

In Figs. 3(b) and 4(b), $\log(f)$ values are plotted against T_{P}^{-1} for peaks A and B, respectively. Linear relations are seen for both peaks, indicating that the two peaks indeed originate in a thermally activated relaxation process. The

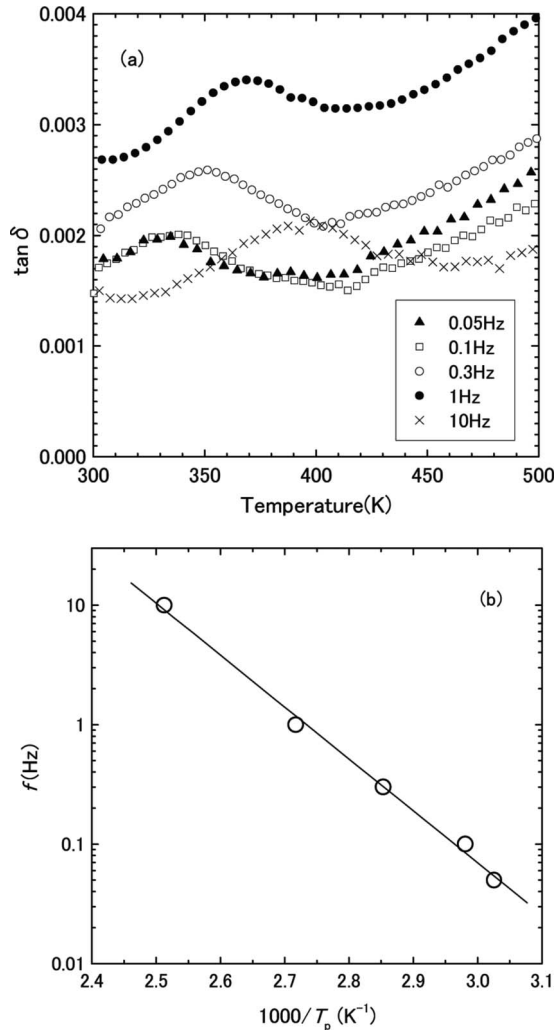


FIG. 3. Temperature dependences of the internal friction at various frequencies for peak A of (a) the polygrained i-phase and (b) the Arrhenius plot of the peak temperature-frequency relation.

thermal activation parameters evaluated for peak A are $\tau_0^{-1} = 1.2 \times 10^{12} \text{ s}^{-1}$ and $H = 0.8 \text{ eV}$, and those for peak B are $5.8 \times 10^{25} \text{ s}^{-1}$ and 4.1 eV .

Figures 5(a)–5(d) show the temperature dependences of the internal friction for peaks C–F of the 2/1-phase at various frequencies, respectively. A shift in the peak position with changes in the frequency can be observed for all the peaks. We determined the peak positions by data fitting. Figure 5(e) shows the Arrhenius plots for the four peaks of the 2/1-phase, from which the activation parameters were evaluated to be $\tau_0^{-1} = 3.0 \times 10^{15} \text{ s}^{-1}$ and $H = 1.0 \text{ eV}$ for C, $9.4 \times 10^{15} \text{ s}^{-1}$ and 1.4 eV for D, $1.3 \times 10^{14} \text{ s}^{-1}$ and 1.8 eV for E, and $1.6 \times 10^{21} \text{ s}^{-1}$ and 3.4 eV for F. The activation parameters for C in the 2/1-phase are roughly the same as those for A in the i-phase. The same is true for peaks B and F.

Figure 6(a) shows the temperature dependences of the internal friction for the 1/1-phase at various frequencies. Peaks G and H both shift toward a high temperature with increasing frequency, and the corresponding Arrhenius plots are shown in Fig. 6(b). The thermal activation parameters were

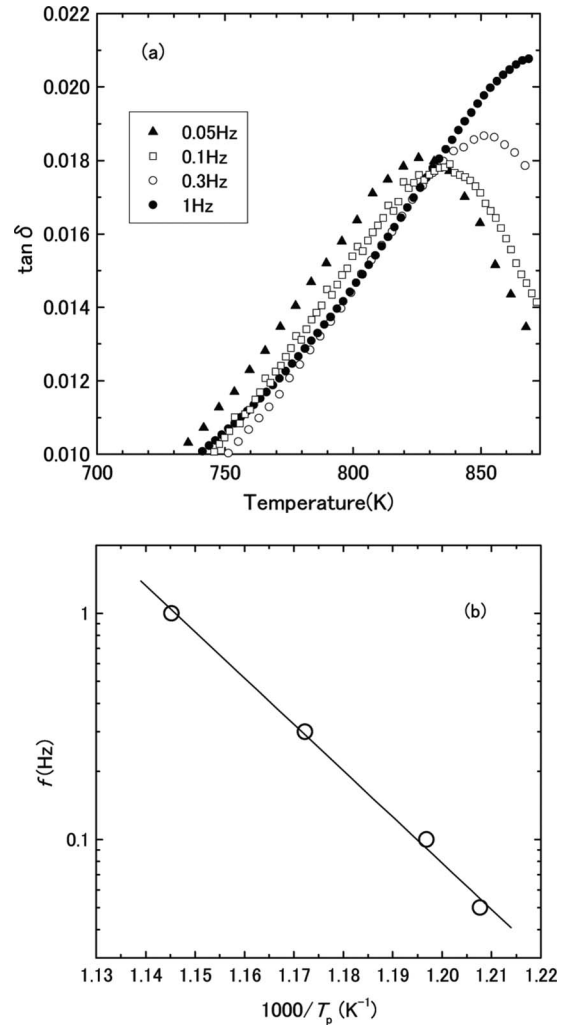


FIG. 4. Temperature dependences of the internal friction at various frequencies for peak B of (a) the polygrained i-phase and (b) the Arrhenius plot of the peak temperature-frequency relation.

evaluated to be $\tau_0^{-1} = 6.2 \times 10^{15} \text{ s}^{-1}$ and $H = 1.8 \text{ eV}$ for peak G, and $1.1 \times 10^{16} \text{ s}^{-1}$ and 2.4 eV for peak H. The activation parameters for the peak G in the 1/1-phase agree well with those for the peak E in the 2/1-phase, indicating that these peaks originate in the same mechanism.

The peak temperature T_p , the thermal activation parameters τ_0^{-1} and H , and the magnitude of the internal friction for the peaks observed for the polygrained samples of the i-phase, 1/1-phase and 2/1-phase are summarized in Table I. Here, we should note the following. First, the internal friction behavior is completely different between the i-phase and the 1/1-phase; peaks A and B observed for the i-phase are absent for the 1/1-phase, and peaks G and H for the 1/1-phase are absent for the i-phase. On the other hand, the 2/1-phase exhibits the features of both the i and 1/1-phases; peaks A and B for the i-phase can be observed for the 2/1-phase, although the intensity of the peaks are reduced, and peak G for the 1/1-phase is also observed for the 2/1-phase, again with a reduced intensity.

Figure 7 shows the temperature dependence of the internal friction for the three single-crystal i-phase samples with

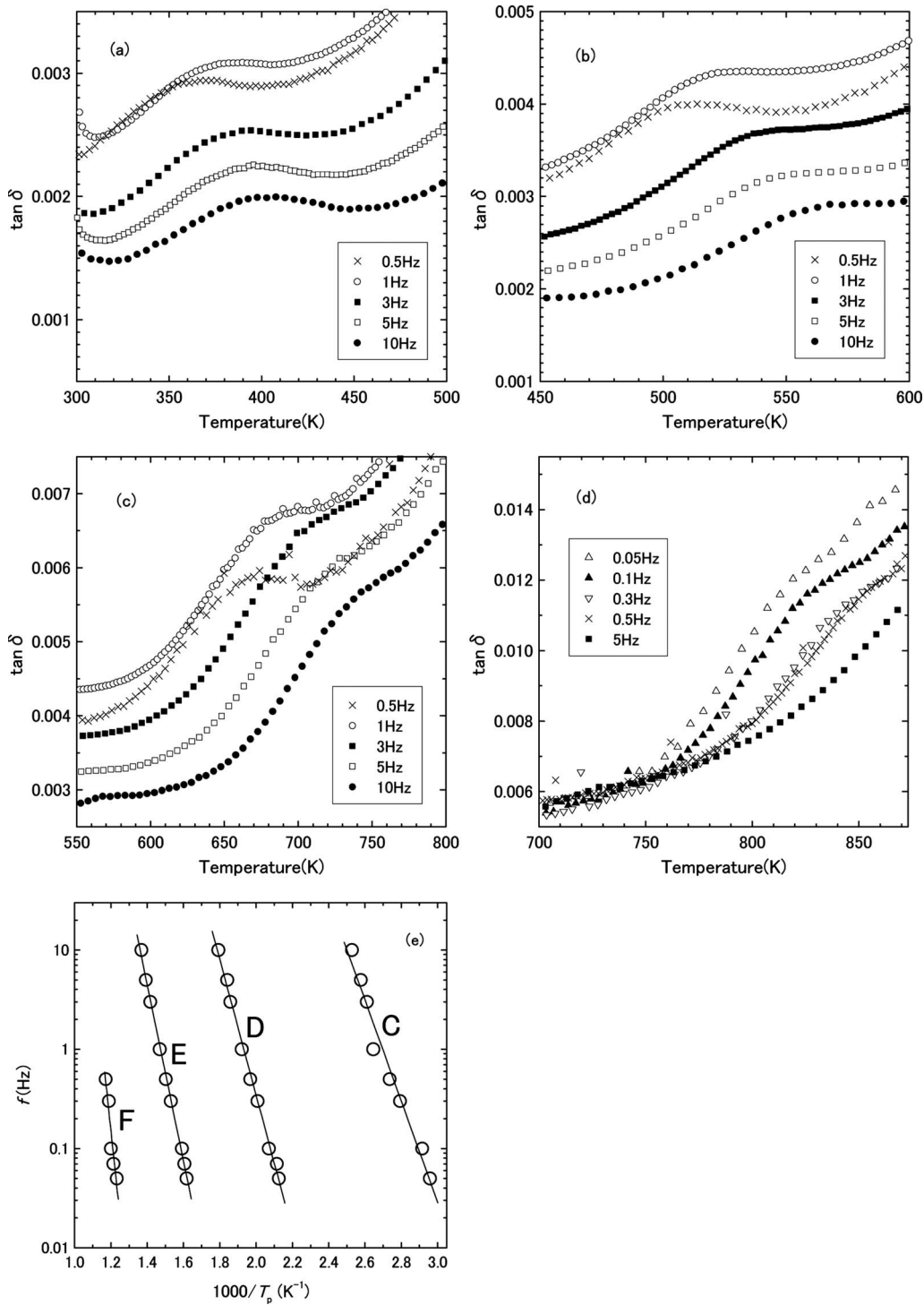


FIG. 5. Temperature dependences of the internal friction at various frequencies for peaks (a) C, (b) D, (c) E, and (d) F of the 2/1-phase, and (e) the Arrhenius plots of the peak temperature-frequency relation.

different crystallographic orientations at a frequency of 0.1 Hz. The three curves agree almost perfectly in the high-temperature region above 600 K. On the other hand, we notice a slight difference in the background level in the low-temperature region below 600 K. However, the background level changes sensitively with the sample-clamping conditions in our experiments, and the slight difference observed in Fig. 4 can be attributed to such a difference in the experi-

mental conditions. Furthermore, no appreciable difference can be observed between the curves shown in Fig. 7 and the curve for the polygrained *i*-phase sample shown in Fig. 2(a). This fact indicates that peaks A and B observed for the polygrained sample in Fig. 1 do not result from the grain boundaries but result entirely from the inside of the grains. Results of thermal activation analyses have shown $\tau_0^{-1} = 10^{14} - 10^{16} \text{ s}^{-1}$ and $H = 1.0 - 1.1 \text{ eV}$ for peak A, and

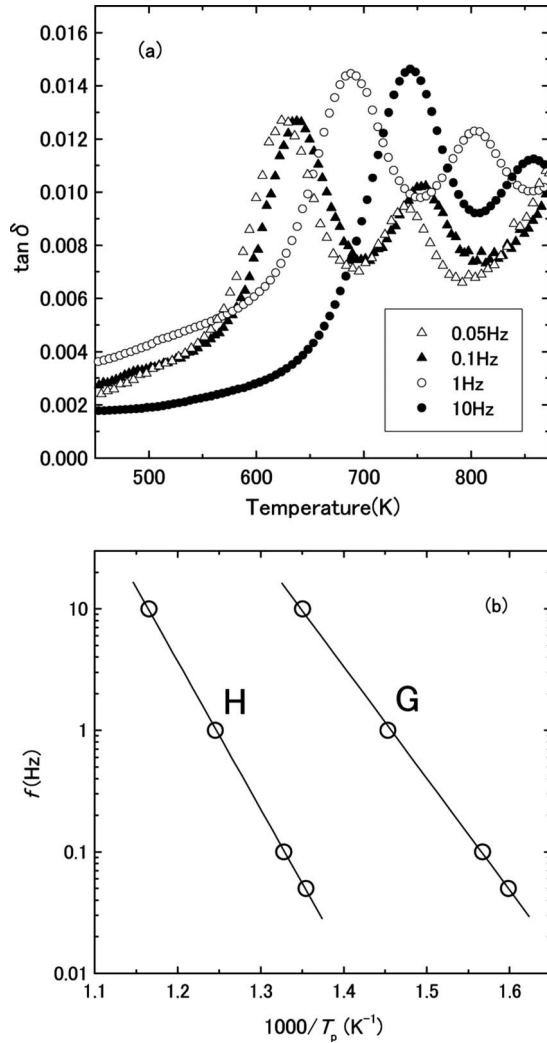


FIG. 6. Temperature dependences of the internal friction at various frequencies for peaks G and H of the (a) 1/1-phase and (b) the Arrhenius plot of the peak temperature-frequency relation.

$\tau_0^{-1} = 10^{20} - 10^{22} \text{ s}^{-1}$ and $H = 3.3 - 3.7 \text{ eV}$ for peak B, which agree with those of the polygrained sample.

IV. DISCUSSION

The temperature dependences of the internal friction for the i-Al-Pd-Mn samples in our experiments [Figs. 2(a) and 7] agree well with those previously reported by Feuerbacher *et al.*^{17,27} The thermal activation parameters τ_0^{-1} and H , which we evaluated for peaks A and B (Table I), are also in good agreement with those reported by them. As pointed out by Feuerbacher *et al.*, the thermal activation parameters of peak A indicate that this peak originates in local jumps of atomic defects; these can be local isolated phason jumps. In our experiments, this peak is absent in the 1/1-phase and present with a reduced intensity in the 2/1-phase. This result is consistent with the results of the quasielastic neutron-scattering experiments performed by Coddens *et al.*²⁸ for i Al-Cu-Fe and its approximant phases; phasonlike atomic jumps were observed for the i-phase and the high-

TABLE I. The peak temperature T_p , the thermal activation parameters τ_0^{-1} and H , and the magnitude of the internal friction δ for the peaks observed for the polygrained samples of the i, 1/1, and 2/1-phases.

| | T_p for $f=0.1 \text{ Hz}$ (K) | τ_0^{-1} (s^{-1}) | H (eV) | $\tan \delta \times 10^{-4}$ | | |
|------|--|--------------------------------------|-------------|------------------------------|--------------|--------------|
| | | | | i phase | 2/1 phase | 1/1 phase |
| A(C) | 330 | $10^{12} - 10^{15}$ | 0.8–1.0 | 8 | 2 | |
| B(F) | 830 | $10^{21} - 10^{25}$ | 3.4–4.1 | 130 | 19 | |
| D | 490 | 10^{15} | 1.4 | | 8 | |
| E(G) | 630 | $10^{14} - 10^{15}$ | 1.8 | | 17 | 88 |
| H | 750 | 10^{16} | 2.4 | | | 38 |

order rhombohedral approximant phase but not for the 1/1-phase.

As shown in Table I, for peak B, the activation enthalpy is large (3.4–4.1 eV) and the frequency factor is also large ($10^{21-25} \text{ s}^{-1}$). Here, the frequency factor is much larger than the Debye frequency ($\approx 10^{13} \text{ s}^{-1}$). These parameters indicate that peak B originates in a relaxation process with a collective atomic motion involving many atoms, as pointed out by Feuerbacher *et al.*¹⁷ Collective and correlated phason jumps are most plausible as the mechanism for it. Phason fluctuations accompanied by collective and correlated phason jumps in i Al-Pd-Mn were investigated by Francoual *et al.*¹¹ using coherent x-ray scattering and time-correlation spectroscopy. They observed the relaxation of phason waves with characteristic times ranging from 20 to 70 s at 923 K, and they evaluated the activation enthalpy to be $3 \pm 1 \text{ eV}$. The relaxation process of the phason wall formed by a dislocation motion in i Al-Pd-Mn was investigated by *in situ* TEM observations by Feuerbacher *et al.*¹² Here, the relaxation of the phason wall requires collective and correlated phason jumps. They reported relaxation times ranging from 0.3 to

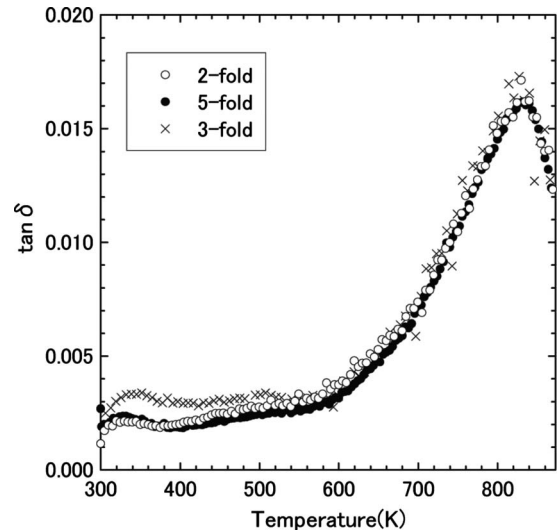


FIG. 7. Temperature dependences of the internal friction for single-crystal samples of i Al-Pd-Mn with different crystallographic orientations at a frequency of 0.1 Hz.

2×10^4 s, obeying an Arrhenius temperature dependence with an activation enthalpy of 4 eV and a frequency factor of 4×10^{21} s $^{-1}$.

In our experiments, peak B was not observed for the 1/1-phase. This fact further supports our interpretation that the origin of peak B was phason fluctuations involving collective and correlated phason jumps. De Boissieu *et al.*²¹ conducted x-ray diffuse scattering measurements for the Zn-Mg-Sc i-phase and its 1/1 approximant phase in the Zn-Sc system, and showed that the diffuse scattering due to phason modes is observed only for the i-phase; it is absent for the 1/1-phase. This fact indicates that the correlated phason fluctuations do not take place in low-order approximant phases such as the 1/1-phase. In principle, as the order of the approximant increases, the unit-cell size of the approximant phase increases and the structure gets close to the quasicrystal. Then, the phason modes should be operative even in an approximant phase, if its order is sufficiently high. As shown in Table. 1, peak B was also observed in the 2/1-phase with a much reduced intensity, which may be a sign of the phason modes operating in a high-order approximant phase.

The elastic energy f of quasicrystals is given as a function of the phonon (conventional) strain $u_{ij} \equiv \frac{1}{2}(\frac{\partial u_i}{\partial r_j} + \frac{\partial u_j}{\partial r_i})$ and the phason strain $w_{ij} \equiv \frac{\partial w_i}{\partial r_j}$, where $\mathbf{u} = [u_1, u_2, u_3]$ and $\mathbf{w} = [w_1, w_2, w_3]$ are the phonon and phason displacement vectors. Within linear elasticity, f comprises the following three types of quadratic terms:⁷⁻⁹

$$f = f_{u-u} + f_{w-w} + f_{u-w} = \frac{1}{2} C_{ijkl}^{u-u} u_{ij} u_{ij} + \frac{1}{2} C_{ijkl}^{w-w} w_{ij} w_{ij} + C_{ijkl}^{u-w} u_{ij} w_{ij}, \quad (4)$$

where f_{u-u} , f_{w-w} , and f_{u-w} are a pure phonon, pure phason, and phonon-phason coupling terms, respectively, and C_{ijkl}^{u-u} , C_{ijkl}^{w-w} , and C_{ijkl}^{u-w} are the corresponding elastic constant tensors. For icosahedral quasicrystals, there are five independent elastic constants: λ and μ (Lame constants) in C_{ijkl}^{u-u} ; K_1 and K_2 in C_{ijkl}^{w-w} ; and K_3 for C_{ijkl}^{u-w} , and the explicit form of each tensor has been derived previously.^{7,9,29}

The internal friction is defined as the dissipation rate of the elastic oscillation energy applied to the system. Here, the elastic oscillation applied to the system is in the pure phonon mode. Therefore, in order for the damping phason waves to be the cause of the internal friction, the phonon oscillation must couple with the phason waves, i.e., the phonon-phason coupling must be nonzero. The internal friction due to the damping phason waves induced by phonon-phason coupling was discussed theoretically by Rochal and Lorman.¹⁶ They investigated the model of the phonon-phason elastodynamics in icosahedral quasicrystals, which obeys the equations

$$\frac{\partial \sigma_{ij}^u}{\partial r_j} = \rho \ddot{u}_i, \quad \frac{\partial \sigma_{ij}^w}{\partial r_j} = D \dot{w}_i, \quad (5)$$

where σ_{ij}^u and σ_{ij}^w are the phonon and phason stress tensors, respectively, ρ is the density, and D is the phason friction coefficient. This model predicts a considerably large anisotropy in the internal friction, as shown in the following. The peak height of internal friction is given as $\frac{I^2}{2\nu K}$, where I de-

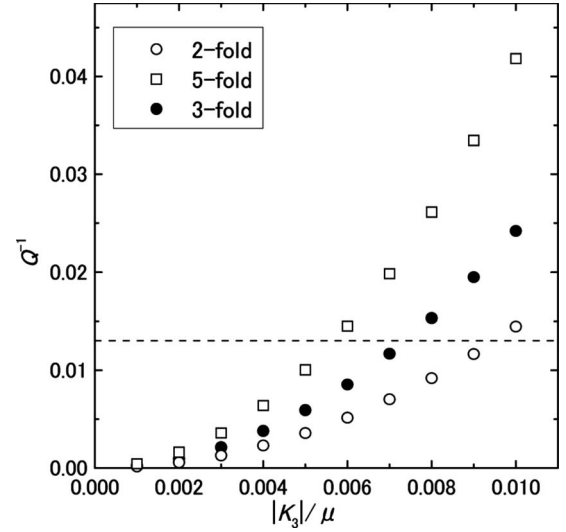


FIG. 8. The peak heights of the internal friction calculated as a function of $|K_3|/\mu$ for different crystallographic orientations. The dashed line represents the Q^{-1} value of peak B in our experiments.

notes the effective phonon-phason coupling constant, and ν and K denote the effective phonon and phason elastic constants, respectively. These effective elastic constants change with changes in the directions of wave vector \mathbf{q} and wave polarization \mathbf{p} of the elastic phonon wave given to the system. In the flexural-oscillation mode in our experiments, an oscillating tension-compression stress is applied along the longitudinal direction of the sample. As a result, oscillating tension-compression stains along the same direction are mainly induced. Then, the induced elastic wave is a longitudinal wave with \mathbf{p} parallel to \mathbf{q} . For the longitudinal waves, $\nu = \lambda + 2\mu$. I and K depend on the direction of $\mathbf{p}(\mathbf{q})$; Rochal and Lorman¹⁶ have derived $I = K_3$ and $K = K_1 - K_2/3$ for the twofold direction, $I = -2K_3$ and $K = K_1 - 4K_2/3$ for the fivefold direction, and $I = 2K_3/3$ and $K = K_1 + 4K_2/3$ for the threefold direction. In Fig. 8, the internal friction peak heights are calculated as a function of $|K_3|/\mu$ using the phonon and phason elastic constants reported previously.^{30,31} Here, the dashed line represents the Q^{-1} value of peak B in our experiments. Figure 8 shows anisotropy by a factor of up to 3. This is inconsistent with our experimental result in which no noticeable anisotropy was observed. In response to the tension-compression stress along the longitudinal direction of the sample, not only the tension-compression strain along this direction but also those along the directions perpendicular to it should be induced, with the magnitudes given by Poisson's ratio. This effect can obscure the anisotropy considerably. Another possibility is that peak B is only partly due to the phason relaxation. Other collective atomic motion such as a dislocation motion could contribute to this peak, although to what degree such a contribution is isotropic is unclear. Feuerbacher and his co-workers²⁷ previously measured internal friction for i-Al-Pd-Mn single-crystal samples with two different crystallographic orientations in a torsional-oscillation mode. They observed no appreciable orientation dependence of the peak height.

If we assume that the height of peak B represents the average value of Q^{-1} for the three directions shown in Fig. 8,

$|K_3|$ can be estimated to be 0.007μ . This value agrees roughly with the estimations of $|K_3|$ previously reported. Zhu and Henley³² calculated K_3 (Γ_{11}^{\pm} in their paper) for model icosahedral quasicrystals of (Al,Cu)-Li and Al-Mn, which belong to the two major classes of the icosahedral phase, namely, the Frank-Kasper and Al transition-metal classes, respectively. They showed that $|K_3|$ is $0.02-0.1\mu$ for (Al,Cu)-Li and $0.003-0.02\mu$ for Al-Mn. Edagawa and So^{33,34} evaluated K_3 experimentally for the Mg-Ga-Al-Zn and Al-Cu-Fe i-phases, which belong to the Frank-Kasper and Al transition-metal classes, respectively, and reported $|K_3|=0.04\mu$ for the former and $|K_3|=0.004\mu$ for the latter. The Al-Pd-Mn i-phase studied in the present work belongs to the Al transition-metal class, and the evaluated value of $|K_3|=0.007\mu$ agrees roughly with those reported by Zhu and Henley, and by Edagawa and So.

Finally, we speculate that the peaks D, E(G), and H observed for the 1/1 and 2/1-phases result from Zener relaxations. The Zener relaxation is a stress-induced reorientation of solute atom pairs, which has been observed in many alloys.³⁵ Atom pairs involving Si atoms may be responsible for those peaks because Si is a constituent only of the approximant phases. The structures of the approximant phases have been determined by x-ray diffraction structural analyses.^{36,37} Because of their complicated structures, it is difficult to determine exactly which atom pairs are responsible for the peaks and what the mechanism is in detail.

V. CONCLUSIONS

The internal friction was measured for an Al-Pd-Mn i-phase and its 1/1 and 2/1 approximant phases in the Al-Pd-Mn-Si system in a forced flexural-oscillation mode in a frequency range of 0.05–20 Hz and a temperature range of 300–873 K. For the i-phase, one large absorption peak and one small absorption peak were observed, with $Q^{-1} \approx 1.3 \times 10^{-2}$

and 8×10^{-4} , respectively. These two peaks were absent for the 1/1-phase, which showed two other peaks instead. The 2/1-phase exhibited the features of both the i and 1/1-phases; it showed two peaks of the i-phase and one of the two peaks of the 1/1-phase. All the observed peaks were of the thermally activated relaxation type, and their activation enthalpies and frequency factors were evaluated. The activation enthalpy and frequency factor evaluated for the larger peak of the i-phase indicated that this peak originates in a relaxation process involving a collective atomic motion. Collective and correlated phason jumps were discussed as a possible mechanism for it. Based on the model of the phonon-phason elastodynamics previously proposed, the magnitude of the phonon-phason coupling constant was estimated to be 0.007μ (μ : shear modulus) from the intensity of the internal friction. This value is in good agreement with the values reported previously. Anisotropy in the internal friction, which is predicted in the model, was not observed. This should be partly due to the sample configuration in our measurements or may indicate that the peak is only partly related to the phason relaxation. It was speculated that the other peaks observed only for the approximant phases are due to Zener relaxations by the reorientation of atom pairs involving Si.

ACKNOWLEDGMENTS

The authors would like to thank S. Takeuchi of Tokyo University of Science (TUS) for the valuable comments and discussion, Y. Kogo of TUS for his help in the internal friction measurements, and T. Iida of TUS for his help in the PAS experiments. This work was financially supported by a Grant-in-Aid for Japan Society for the Promotion of Science (JSPS) and by a Grant-in-Aid for Scientific Research on Priority Areas “Nano Materials Science for Atomic Scale Modification 474,” from the Ministry of Education, Culture, Sports, Science and Technology (MEXT) of Japan.

*FAX: +81-3-5452-6106; so@iis.u-tokyo.ac.jp

¹D. Levine and P. J. Steinhardt, Phys. Rev. B **34**, 596 (1986).

²J. E. S. Socolar and P. J. Steinhardt, Phys. Rev. B **34**, 617 (1986).

³P. J. Steinhardt and S. Ostlund, *The Physics of Quasicrystals* (World Scientific, Singapore, 1987).

⁴D. Shechtman, I. Blech, D. Gratias, and J. W. Cahn, Phys. Rev. Lett. **53**, 1951 (1984).

⁵A. P. Tsai, Sci. Technol. Adv. Mater. **9**, 013008 (2008).

⁶J. E. S. Socolar, T. C. Lubensky, and P. J. Steinhardt, Phys. Rev. B **34**, 3345 (1986).

⁷D. Levine, T. C. Lubensky, S. Ostlund, S. Ramaswamy, P. J. Steinhardt, and J. Toner, Phys. Rev. Lett. **54**, 1520 (1985).

⁸P. Bak, Phys. Rev. B **32**, 5764 (1985).

⁹T. C. Lubensky, S. Ramaswamy, and J. Toner, Phys. Rev. B **32**, 7444 (1985).

¹⁰M. de Boissieu, R. Currat, and S. Francoual, in *Quasicrystals*, edited by T. Fujiwara and Y. Ishii (Elsevier Science B.V., Oxford, 2007), p. 107.

¹¹S. Francoual, F. Livet, M. de Boissieu, F. Yakhou, F. Bley, A. Letoublon, R. Caudron, and J. Gastaldi, Phys. Rev. Lett. **91**, 225501 (2003).

¹²M. Feuerbacher and D. Caillard, Acta Mater. **54**, 3233 (2006).

¹³K. Edagawa, K. Suzuki, and S. Takeuchi, Phys. Rev. Lett. **85**, 1674 (2000).

¹⁴K. Edagawa, K. Suzuki and S. Takeuchi, J. Alloys Compd. **342**, 271 (2002).

¹⁵K. Edagawa, P. Mandal, K. Hosono, K. Suzuki, and S. Takeuchi, Phys. Rev. B **70**, 184202 (2004).

¹⁶S. B. Rochal and V. L. Lorman, Phys. Rev. B **66**, 144204 (2002).

¹⁷M. Feuerbacher, M. Weller, J. Diehl, and K. Urban, Philos. Mag. Lett. **74**, 81 (1996).

¹⁸V. Elser and C. L. Henley, Phys. Rev. Lett. **55**, 2883 (1985).

¹⁹C. L. Henley and V. Elser, Philos. Mag. B **53**, L59 (1986).

²⁰M. Aduier and P. Guyot, *Extended Icosahedral Structures* (Academic, San Diego, CA, 1989), p. 1.

²¹M. de Boissieu, S. Francoual, Y. Kaneko, and T. Ishimasa, Phys. Rev. Lett. **95**, 105503 (2005).

- ²²V. Elser, Phys. Rev. B **32**, 4892 (1985).
- ²³Y. G. So, A. Shimizu, K. Edagawa, and S. Takeuchi, Philos. Mag. **86**, 373 (2006).
- ²⁴N. Koshikawa, S. Yoda, K. Edagawa, M. Ohtsuki, and S. Takeuchi, Philos. Mag. Lett. **83**, 205 (2003).
- ²⁵M. Weller, H. Clements, and G. Haneczok, Mater. Sci. Eng., A **442**, 138 (2006).
- ²⁶Z. C. Zhou and F. S. Han, Phys. Status Solidi A **199**, 202 (2003).
- ²⁷M. Feuerbacher, M. Weller, and K. Urban, in Proceedings of the 6th International Conference on Quasicrystals, edited by S. Takeuchi (World Scientific, Singapore, 1998), p. 521.
- ²⁸G. Coddens, S. Lyonnard, and Y. Calvayrac, Phys. Rev. Lett. **78**, 4209 (1997).
- ²⁹M. Widom, Philos. Mag. Lett. **64**, 297 (1991).
- ³⁰K. Tanaka, Y. Mitarai, and M. Koiwa, Philos. Mag. A **73**, 1715 (1996).
- ³¹A. Letoublon, M. de Boissieu, M. Boudard, L. Mancini, J. Gastaldi, B. Hennion, R. Caudron, and R. Bellissent, Philos. Mag. Lett. **81**, 273 (2001).
- ³²W.-J. Zhu and C. L. Henley, Europhys. Lett. **46**, 748 (1999).
- ³³K. Edagawa, Philos. Mag. Lett. **85**, 455 (2005).
- ³⁴K. Edagawa and Y. G. So, Philos. Mag. **87**, 77 (2007).
- ³⁵A. S. Nowick and B. S. Berry, *Anelastic Relaxation in Crystal-line Solids* (Academic, New York, 1972).
- ³⁶K. Sugiyama, N. Kaji, K. Hiraga, and T. Ishimasa, Z. Kristallogr. **213**, 168 (1998).
- ³⁷K. Sugiyama, N. Kaji, K. Hiraga, and T. Ishimasa, Z. Kristallogr. **213**, 90 (1998).